Supported Vanadium Oxide Catalysts: Quantitative Spectroscopy, Preferential Adsorption of $V^{4+/5+}$, and Al_2O_3 Coating of Zeolite Y

Gabriela Catana,[†,§] R. Ramachandra Rao,[†] Bert M. Weckhuysen,*[,†] Pascal Van Der Voort,[‡] Etienne Vansant,[‡] and Robert A. Schoonheydt[†]

Centrum voor Oppervlaktechemie en Katalyse, Departement Interfasechemie, K.U.Leuven, Kardinaal Mercierlaan 92, 3001 Heverlee, Belgium, and Laboratorium voor Anorganische Scheikunde, Departement Scheikunde, U.I.Antwerpen, Universiteitsplein 1, 2610 Wilrijk, Belgium

Received: March 13, 1998; In Final Form: May 12, 1998

A series of supported vanadium oxide catalysts were prepared by the incipient wetness method as a function of the support composition (Al_2O_3, SiO_2, and USY), the metal oxide loading (0−1 wt %), and the impregnation salt (vanadyl sulfate and ammonium vanadate). These catalysts have been studied by combined DRS-ESR spectroscopies in order to quantify the amount of V^{4+} and V^{5+} and to unravel their coordination geometries. These spectroscopic fingerprints have been used to study the preferential adsorption of $V^{4+/5+}$ ions on SiO_2, Al_2O_3, and USY. Both V^{4+} and V^{5+} were preferentially adsorbed on Al_2O_3 and showed a much smaller preference for USY and SiO_2. The observed preference orders are discussed in relation with the properties of the support. In addition, a novel method is proposed to coat the external surface of USY with a thin film of Al_2O_3. The method is based on the deposition of USY with the so-called Keggin ion, $[Al_{13}O_4(OH)_{24}(H_2O)_{12}]^{7+}$, which is too big to enter the USY channels or pores. The obtained Al_2O_3/USY material showed a preferential adsorption of V^{4+} onto the Al_2O_3 film, suggesting that this method could be useful for vanadium passivation of FCC catalysts.

1. Introduction

Supported vanadium oxide catalysts have found wide commercial application as oxidation catalysts, e.g., for the selective oxidation of *o*-xylene to phthalic anhydride, ammoxidation of alkyl aromatics, selective catalytic reduction (SCR) of NO_x with NH_3, and controlling the oxidation of SO_2 to SO_3 during SCR.[1−5] Furthermore, supported vanadium oxide catalysts are active in the oxidative dehydrogenation of alkanes to olefins, oxidation of butane to maleic anhydride, and the selective oxidation of methanol to formaldehyde or methyl formate.[6,7] In addition, vanadium oxides are generally known as a poison for fluid catalytic cracking (FCC) catalysts by destroying the Brönsted acid sites and the structure of the ultrastable zeolite Y (USY).[8−10] This implies the presence of highly mobile vanadium oxide species.

A prerequisite for understanding the behavior of supported vanadium oxide catalysts is a thorough knowledge of their surface chemistry and reactivity as a function of the type and composition of the supports and of the environmental conditions. Despite numerous—mostly qualitative—characterization studies, many fundamental questions concerning the oxidation states and coordination geometries of surface vanadia species still remain unanswered, and this has been the subject of a recent review.[11]

The goal of this paper is 2-fold: The first is to use a combination of diffuse reflectance spectroscopy (DRS) and electron spin resonance (ESR) to quantify the amount of supported V^{4+} and V^{5+} and to unravel their coordination geometries. Both spectroscopies have been shown to be very useful for the characterization of other supported metal oxide catalysts.[12−14] The second goal is to use the obtained spectroscopic fingerprints to study the preferential adsorption of $V^{4+/5+}$ ions onto SiO_2, Al_2O_3, and USY. In addition, a novel method is proposed to coat the external surface of USY with a thin film of Al_2O_3. The method is based on the deposition of USY with the so-called Keggin or Al_{13} ion, $[Al_{13}O_4(OH)_{24}(H_2O)_{12}]^{7+}$, which is too big to enter the USY channels or pores. It will be shown that V^{4+} ions preferentially adsorb onto this Al_2O_3 film.

2. Experimental Section

1. Sample Preparation and Characteristics. The following supports were used in this study: USY (CBV780, PQ Corporation) with a Si:Al ratio of 20, NaY (Zeocat) with a Si:Al ratio of 2.4, SiO_2 (Degussa), Al_2O_3 (Merck), Al_{13}-coated USY (see further), and physical mixtures (50/50) of USY and Al_2O_3, USY and SiO_2, and Al_2O_3 and SiO_2. These mixtures were obtained by mixing equal amounts of these supports in a mortar for 15 min. Supported vanadium oxide catalysts were prepared by the incipient wetness technique with aqueous solutions of vanadyl sulfate ($VOSO_4 \cdot H_2O$, Janssen Chimica) or ammonium vanadate (NH_4VO_3, Janssen Chimica).

2. Preparation of the Keggin Al_{13} Ion and Al_{13} Coating of USY. The Keggin Al_{13} ion was prepared according to the method of Furrer et al.[15,16] A 250 mL aliquot of a 0.25 M $AlCl_3$ solution (UCB) was heated in a water bath to 80 °C. Then, 600 mL of a 0.25 M NaOH solution (Janssen Chimica) was added at a rate of 4 mL/min while stirring at 300 rpm. After cooling this solution, 625 mL of 0.1 M Na_2SO_4 (UCB) was added, and during continuous stirring at 830 rpm a precipitate was formed over a 2 day period. This precipitate, $[Al_{13}O_4$-

[†] Centrum voor Oppervlaktechemie en Katalyse.
[‡] Laboratorium voor Anorganische Scheikunde.
[§] On leave from the National Institute of Materials Physics, Bucharest, Romania.
* To whom correspondence should be addressed.

S1089-5647(98)01482-5 CCC: $15.00
Published on Web 09/19/1998

TABLE 1: Band Maxima of DRS Spectra of Some Reference Compounds and Supported Vanadium Oxide Catalysts

compd	DRS absorption max (nm)[a]	oxidation state	mol struct[b]
NH_4VO_3	362, 286, 219	5+	metavanadate: T_d and polymeric
Na_3VO_4	352, 282, 228	5+	orthovanadate: T_d and isolated
$Pb_2V_2O_7$	361, 266, 217	5+	pyrovanadate: T_d and dimeric
ZnV_2O_6	487, 269, 220	5+	O_h and dimeric
V_2O_5	477, 325, 240	5+	O_h and polymeric
$Na_6V_{10}O_{28}$	414 (sh), 289, 210	5+	O_h and polymeric
V_2O_4	1283 (br), 355, 240	4+	O_h and rutile structure
$VOSO_4 \cdot 2H_2O$	747, 654, 266, 210	4+	square pyramidal and isolated
$VO(acac)_x$	694, 601 (sh), 378, 272	4+	square pyramidal and isolated
$VO(H_2O)_5^{2+}$	770, 629, 366	4+	O_h and isolated
V^{4+}/Al_2O_3	805, 580, 275	4+	O_h and isolated
V^{4+}/SiO_2	770, 625, 325	4+	O_h and isolated
V^{4+}/USY	770, 625, 425	4+	O_h and isolated
V^{5+}/Al_2O_3	370 (sh), 272 (sh)	5+	T_d
V^{5+}/SiO_2	340	5+	T_d
V^{5+}/USY	405	5+	T_d and some polymeric $V^{5+}(O_h)$

[a] sh, shoulder; br, broad; T_d, tetrahedral; and O_h, octahedral. [b] References 18−20.

$(OH)_{24}(H_2O)_{12}][(SO_4)_{7/2}]$, was filtered off, washed with distilled water, and freeze-dried. The obtained precipitate was redissolved with $Ba(NO_3)_2$ (Merck) in 1200 mL of H_2O in an ultrasonic bath for 4 h. The solution was separated from the precipitated $BaSO_4$ by filtration (0.1 μm, Millipore) and centrifugation at 11 000 rpm for 15 min.

Al_{13}-coated USY zeolite was obtained by ion exchanging 5 g of USY zeolite at room temperature for 24 h in a 340 mL solution of Al_{13}. The solid product was separated by centrifugation, followed by washing and drying. The dried material was then calcined overnight in air at 500 °C. This material is denoted as [Al_{13}]-USY. Successive ion exchanges of this material with Al_{13} resulted in Al_{13}-enriched USY materials, denoted as $[Al_{13}]_x$-USY (with x, the number of ion exchanges). The obtained materials were calcined overnight in air at 500 °C between each ion-exchange step.

3. Pretreatment and Experimental Techniques. The supported vanadium oxide catalysts were granulated, and the size fraction 0.25−0.4 mm was loaded in a quartz cell with Suprasil window for DRS and a sidearm for ESR. DRS spectra were taken with a Varian Cary 5 UV−vis−NIR spectrometer at room temperature. The spectra were recorded against a halon white reflectance standard in the range 200−2500 nm. The computer processing of the spectra consisted of the following steps: (1) subtraction of the baseline, (2) conversion to wavenumber, and (3) calculation of the Kubelka−Munk (KM) function. ESR spectra were taken with a Bruker ESP300E spectrometer in X-band (9.5 GHz) with a double rectangular TE_{104} mode cavity. The modulation frequency and amplitude were 100 kHz and 5 G, respectively. The ESR spectra were simulated with the QPOW program of the University of Illinois at Urbana-Champaign.[17]

X-ray powder diffractograms were obtained using a Siemens D5000 X-ray diffractometer (XRD) with Cu Kα radiation. Liquid ^{27}Al nuclear magnetic resonance (NMR) measurements were performed with a Bruker AMX 300 spectrometer at 78.208 MHz, with a pulse length of 6 μs and a pulse delay of 5 s. $Al(OH)_4^-$ in D_2O was used as a reference with a single resonance at 80 ppm. ^{27}Al magic angle spinning (MAS) NMR of the solid samples was measured on a Bruker MSL 400 spectrometer at 104.2 MHz with a pulse length of 0.61 μs and pulse delay of 0.1 s. Na and Al analyses were done with a Varian Spectra AA-20 Plus spectrometer, whereas electron microprobe surface analysis was performed on a JEOL Superprobe 733 microscope. Scanning electron microscopy (SEM) was performed with a Phillips 515 microscope. The samples were suspended in acetone and ultrasonic treated for 15 min. One droplet of suspension was coated on an alumina support. The coated support was covered by a gold film after drying and in vacuo treatment. Surface areas of zeolite USY and Al_2O_3-coated zeolite USY were measured by dynamic N_2 adsorption on an Omnisorp 100 (Coulter), after pretreatment in a vacuum at 200 °C for 8 h.

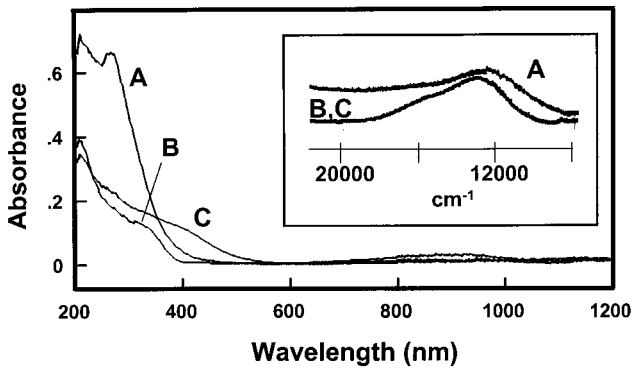

Figure 1. DRS spectra of air-dry 0.1 wt % V^{4+} catalysts as a function of the support type: (A) Al_2O_3, (B) SiO_2, and (C) USY.

3. Results

1. Qualitative Spectroscopy. The DRS spectra of vanadium oxides are characterized by charge-transfer (CT) transitions of the type $O \rightarrow V^{n+}$ and d−d transitions of V^{n+}, and their energies are dependent on the oxidation state and coordination environment. This is illustrated in Table 1 for several reference compounds of V^{4+} and V^{5+}. It is clear that the band maxima of the CT transitions of V^{5+} shift to higher energy (lower nanometers) with decreasing coordination number. It is also clear that because DRS only probes the first coordination environment, the obtained information about the polymerization degree of V^{5+} is rather limited. Thus, the polymerization of $V^{5+}(T_d)$ is only evidenced by a broadening of the absorption bands and/or a small shift of the absorption maxima to lower energy (higher nanometers).

The DRS band maxima of freshly prepared vanadium oxide catalysts depend on the support composition (Al_2O_3, SiO_2, and USY), the vanadium loading (0−1 wt %), and the impregnation salt (NH_4VO_3 and $VOSO_4$) (Table 1). Figure 1 compares the DRS spectra of 0.1 wt % V^{4+}/SiO_2, Al_2O_3, and USY catalysts. Although the spectra are quite similar, one can notice some important differences both in the d−d region and the UV region.

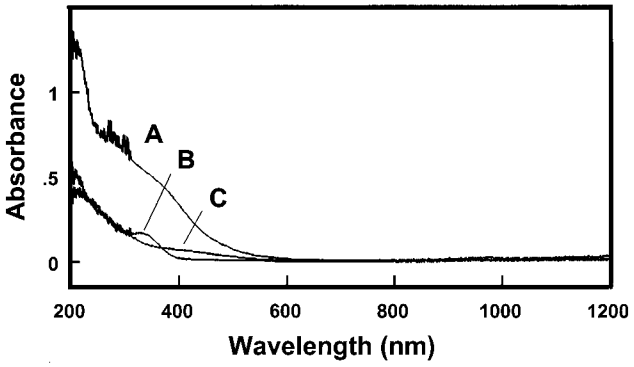

Figure 2. DRS spectra of air-dry 0.1 wt % V^{5+} catalysts as a function of the support type: (A) Al_2O_3, (B) SiO_2, and (C) USY.

In the d−d region (see insert in Figure 1), the V/USY and V/SiO_2 samples are characterized by a weak absorption band and a shoulder at 770 nm (12 990 cm^{-1}) and 625 nm (16 000 cm^{-1}), respectively. In the case of V/Al_2O_3 catalysts, the absorption band and shoulder are shifted to 805 nm (12 420 cm^{-1}) and 580 nm (17 240 cm^{-1}), respectively. Both transitions are typical for V^{4+} in pseudooctahedral coordination (Table 1). The UV region is more complex, and the CT transition of V^{4+} is located at 275 and 325 nm for V^{4+}/Al_2O_3 and V/SiO_2, respectively. In the case of V^{4+}/USY, a broad ill-defined absorption maximum is observed at around 425 nm. It is also important to notice that no additional absorption bands were observed at higher V loadings, suggesting that the same V^{4+} species is present within the 0−1.0 wt % V range. Finally, the absorption at around 200 nm has to be addressed. This intense and relatively broad band is due to a CT transition of the support, being either Al_2O_3, SiO_2, or USY.

The DRS spectra of 0.1 wt % V^{5+}/USY, SiO_2 and Al_2O_3 catalysts are given in Figure 2. The DRS spectrum of V^{5+}/SiO_2 is characterized by an intense band at around 340 nm, which is typical for V^{5+} in tetrahedral coordination (Table 1). However, as discussed above, our DRS measurements do not allow to clearly distinguish between monomeric and polymeric $V^{5+}(T_d)$. In the case of V^{5+}/Al_2O_3, a broad absorption band is visible with a shoulder located at around 370 nm. This shoulder is shifted to 405 nm for V^{5+}/USY samples. Thus, V^{5+} is present in tetrahedral coordination on Al_2O_3, whereas some polymeric $V^{5+}(O_h)$ is detected on USY (Table 1). Similar DRS spectra are obtained for V^{5+} catalysts with higher V loadings, and only for the 1.0 wt % V^{5+}/SiO_2 sample, an additional shoulder became visible at 450 nm. This shoulder is assigned to polymeric $V^{5+}(O_h)$.

The ESR spectra of 0.1 wt % V^{4+} on Al_2O_3, SiO_2, and USY are presented in Figure 3. Such spectra are typical for V^{4+}, with a d^1 configuration and a nuclear spin I of $^7/_2$, resulting in a complex spectrum with a high number of hyperfine lines. Similar spectra were obtained for other V loadings, although for the highest V loading of 1.0 wt % an additional broad signal with g around 2.0 is observed. The latter signal is most probably due to clustered V^{4+}. Thus, at relatively low loadings only one V^{4+} ESR signal is observed for each support. To get more insight into the coordination geometry of dispersed V^{4+}, we have simulated the ESR spectra according to the following spin Hamiltonian H[14]:

$$H = \beta[g_{xx}B_{xx}S_{xx} + g_{yy}B_{yy}S_{yy} + g_{zz}B_{zz}S_{zz}] + [A_{xx}S_{xx}I_{xx} + A_{yy}S_{yy}I_{yy} + A_{zz}S_{zz}I_{zz}] \quad (1)$$

with β, the electronic Bohr magneton; **B**, the magnetic field; g, the effective g value for the x, y, and z direction; **S**, the electron spin angular momentum vector in the x, y, and z direction; **A**; the hyperfine coupling tensor in the x, y, and z direction; and **I**, the nuclear spin angular momentum vector in the x, y, and z direction. The obtained g and A values and the corresponding line widths are summarized in Table 2. It is clear that the g and A values are slightly rhombic, which is indicative of V^{4+} in a distorted symmetry.

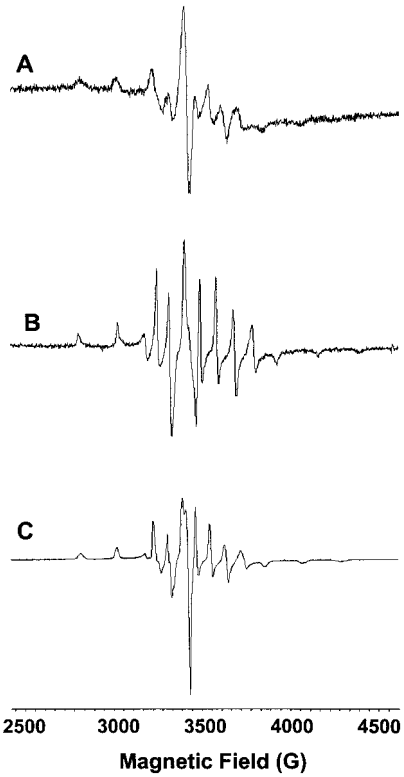

Figure 3. ESR spectra of air-dry 0.1 wt % V^{4+} catalysts as a function of the support type: (A) Al_2O_3, (B) SiO_2, and (C) USY.

2. Quantitative Spectroscopy. DRS spectroscopy allows a quantitative determination of supported V^{n+} ions, according to[12,13]

$$\text{K−M}(V^{n+}) = \frac{(1 - R_\infty)^2}{2R_\infty} = \frac{K}{S} = kC_{V^{n+}} \quad (2)$$

with R_∞, the diffuse reflection of the sample; K, an apparent absorption coefficient; S, an apparent scattering coefficient; k, a proportionality constant; and $C_{V^{n+}}$, the amount of V^{n+}. By plotting the $K-M$ intensity of the d−d transition of V^{4+} at 770 nm (USY and SiO_2) or 805 nm (Al_2O_3) as a function of the V loading, one can obtain a set of calibration lines for supported V^{4+} species. This is illustrated in Figure 4, which shows an almost linear increase of the K−M intensity with increasing V loading for V/Al_2O_3 catalysts. In the case of V^{4+}/USY and V^{4+}/SiO_2 samples, the K−M intensity linearly increases with V loading up to 0.2 wt %, but the calibration lines deviate from linearity at higher V loadings. A comparable set of calibration lines could be established for V^{5+} (Figure 5). Also here, the K−M intensity of the CT transfer of V^{5+} linearly increases with increasing V loading but deviates from linearity for the highest V loading.

The ESR technique can also be used to quantify supported V^{4+} ions. This is illustrated in Figure 6A, which shows the ESR intensity of V^{4+}, obtained by double integration of the spectra, as a function of the V loading. It is clear that the ESR

TABLE 2: ESR Parameters of Supported Vanadium Oxide Catalysts

support	g_{xx}	g_{yy}	g_{zz}	A_{xx} (G)	A_{yy} (G)	A_{zz} (G)	w_{xx} (G)	w_{yy} (G)	w_{zz} (G)	g_{iso}	A_{iso} (G)	$\|\Delta g_{\perp}\|$
SiO_2	1.958	1.988	1.948	71.6	93.5	203.7	22	28	22	1.965	122.9	
Al_2O_3	1.985	1.983	1.947	84.9	89.9	209.3	35	45	35	1.972	128.0	0.0183
USY	1.984	1.981	1.936	77.1	72.8	197.2	30	35	30	1.967	115.7	0.0193

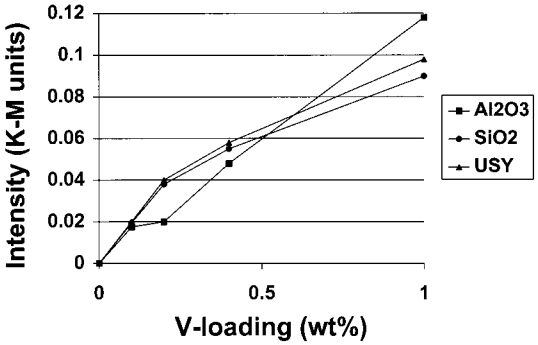

Figure 4. DRS intensities of the d−d transition of V^{4+} for supported vanadium oxide catalysts as a function of the support type (Al_2O_3, SiO_2, and USY) and V loading (0−1 wt %).

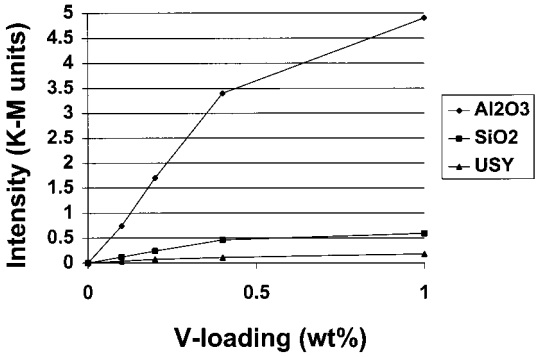

Figure 5. DRS intensities of the CT transition of V^{5+} for supported vanadium oxide catalysts as a function of the support type (Al_2O_3, SiO_2, and USY) and V loading (0−1 wt %).

intensity linearly increases with increasing V loading up to 0.4 wt %. Here again, the intensity plots deviate from linearity for the samples with the highest V loading. The comparison between the DRS and ESR intensities for different V^{4+}/Al_2O_3 catalysts, as given in Figure 6B, suggests that both spectroscopies probe the same V species, and thus in essence the same chemical information is obtained. The deviation from linearity at higher loadings is mainly due to the presence of some clustered V^{4+} in ESR.

Summarizing, combined DRS−ESR spectroscopies allow a quantitative determination of supported V^{4+} and V^{5+} ions, at least at low V loadings. However, the ESR spectra are much better resolved, which makes ESR the technique of choice to quantify the amount of V^{4+}.

3. Preferential Adsorption and Mobility. When two supports are in competition for $V^{4+/5+}$, the latter may preferentially go to the support with which it has the strongest affinity. It is this competition which is studied in this section, and the spectroscopic fingerprints of $V^{4+/5+}$, obtained by combined DRS−ESR spectroscopies, will be used to evaluate preferential adsorption and mobility. The following physical mixtures (50/50) were studied: Al_2O_3/SiO_2, Al_2O_3/USY, and SiO_2/USY.

The DRS spectra of air-dry V^{5+}- and V^{4+}-impregnated Al_2O_3/SiO_2, Al_2O_3/USY, and SiO_2/USY are given in Figures 7 and 8. It is clear that for the physical mixtures Al_2O_3/USY and Al_2O_3/SiO_2 the DRS spectra are Al_2O_3-like (Table 1). Thus, both V^{4+} and V^{5+} ions preferentially adsorb onto Al_2O_3 surfaces. In the case of physical mixtures of USY and SiO_2, the spectra are more

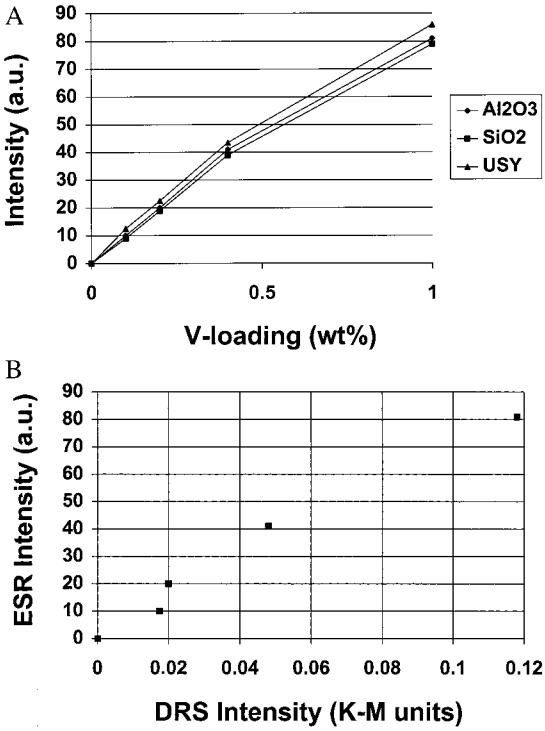

Figure 6. (A, top) ESR intensities of the V^{4+} signal, obtained by double integration of the spectra, for supported vanadium oxide catalysts as a function of the support type (Al_2O_3, SiO_2, and USY) and V loading (0−1 wt %). (B, bottom) Comparison between the DRS and ESR intensities of V^{4+} on Al_2O_3.

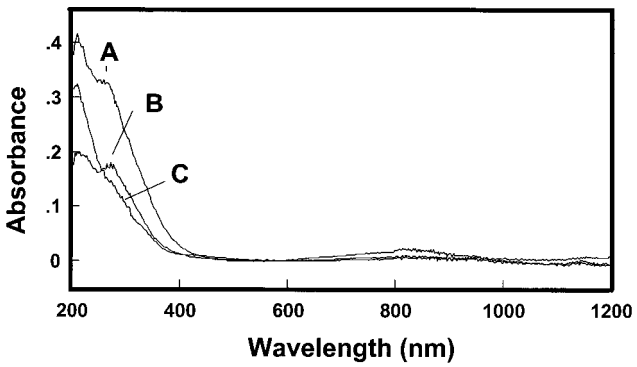

Figure 7. DRS spectra of air-dry 0.1 wt % V^{4+} catalysts for different physical mixtures: (A) Al_2O_3/SiO_2, (B) Al_2O_3/USY, and (C) SiO_2/USY.

SiO_2-like (Table 1), suggesting the preferential adsorption of V^{4+} and V^{5+} onto SiO_2.

The ESR spectra of the air-dry V^{4+}-impregnated Al_2O_3/SiO_2, Al_2O_3/USY, and SiO_2/USY are shown in Figure 9. Also here, the ESR spectra of V^{4+}-impregnated physical mixtures containing Al_2O_3 are clearly Al_2O_3-like (Table 2). On the other hand, the V^{4+}/SiO_2/USY sample has a complex overlapping spectrum, and V^{4+} is assumed to be mainly located at both SiO_2 and USY. Because USY contains Al some preference may also exist for this support. Thus, combined DRS−ESR spectroscopies indicate the following preference order for $V^{4+/5+}$ ions: Al_2O_3 > $SiO_2 \cong$ USY. The same sequence has been observed for $Cr^{5+/6+}$.[21]

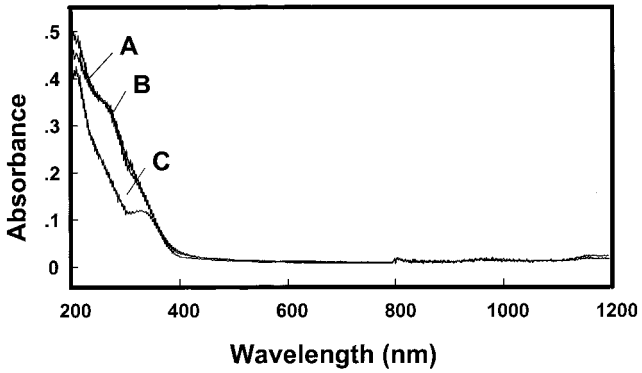

Figure 8. DRS spectra of air-dry 0.1 wt % V^{5+} catalysts for different physical mixtures: (A) Al_2O_3/SiO_2, (B) Al_2O_3/USY, and (C) SiO_2/USY.

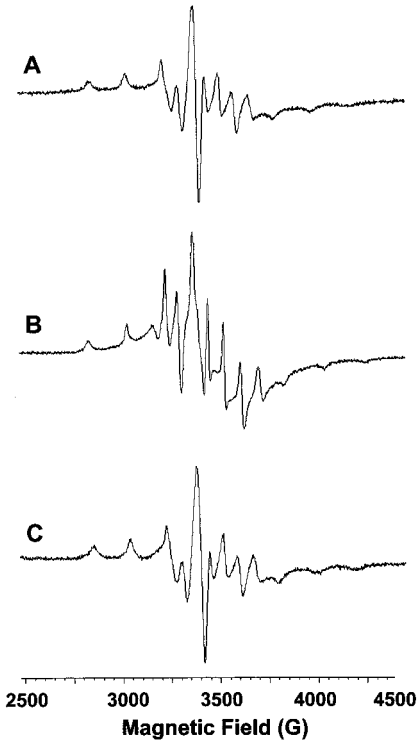

Figure 9. ESR spectra of air-dry 0.1 wt % V^{4+} catalysts for different physical mixtures: (A) Al_2O_3/SiO_2, (B) SiO_2/USY, and (C) Al_2O_3/USY.

4. Al_2O_3 Coating of Zeolite Y. Because of the preferential adsorption of $V^{4+/5+}$ onto Al_2O_3, one could try to coat the external surface of USY with a thin film of Al_2O_3 to obtain a material possibly useful for vanadium passivation in FCC processes. We propose here a novel method based on the deposition of USY with the so-called Keggin or Al_{13} ion, $[Al_{13}O_4(OH)_{24}(H_2O)_{12}]^{7+}$. This complex has a Keggin structure with one tetrahedral Al surrounded by 12 octahedral Al atoms and is too big to enter the zeolite channels or pores.

The aqueous ion-exchange solution, prepared according to the method of Furrer et al.,[15] showed in the corresponding ^{27}Al NMR spectrum only one peak at 62.5 ppm of tetrahedral Al^{3+} in the center of a Keggin structure, which confirms the presence and stability of the Al_{13} ion. By using an increasing amount of Al_{13} in the ion-exchange solution together with NaY or USY, we have measured the amount of released Na^+, together with the amount of Al_{13} taken up by the zeolite material. These results are presented in Figure 10 for NaY. The amount of Al_{13} taken up by the zeolite material gradually increases with increasing amount of Al_{13} in the exchange solution but levels off at around 0.88 and 0.11 mmol of Al/g for NaY and USY,

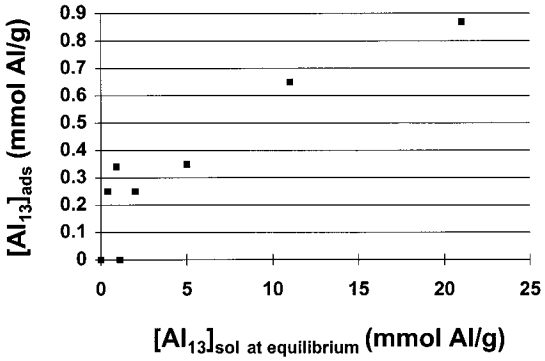

Figure 10. Amount of Al_{13} taken up by the zeolite NaY as a function of the amount of Al_{13} in the exchange solution.

respectively. The deposition of Al_{13} onto the zeolite surface was then verified by ^{27}Al MAS NMR, which showed the presence of a peak at 0 ppm in the Al_{13}-exchanged materials, which can be ascribed to octahedral Al^{3+}. This peak at 0 ppm was increasing in intensity with increasing amount of Al_{13} in the initial exchange solution.

To have higher amounts of Al_2O_3 coating on USY, the $[Al_{13}]$-USY material was first calcined at 500 °C and then ion exchanged again. This procedure was repeated up to five times, and the obtained $[Al_{13}]_2$-USY and $[Al_{13}]_5$-USY materials were characterized by electron microprobe surface analysis. We found a gradual increase/decrease of the amount of Al/Na at the zeolite surface with increasing amount of adsorbed Al_{13}. This is indicative for the deposition of Al onto the external surface of the zeolite. Furthermore, the XRD patterns of $[Al_{13}]_x$-USY materials were identical to those of the pure USY material, although for the highest Al_{13} coatings some amorphous background could be observed. To study the possible changes in morphology of the samples, we have applied scanning electron microscopy (SEM), and the obtained scanning electron micrographs revealed that there was—within the experimental detection limits—no formation of Al_2O_3 agglomerates or lattice destruction. Finally, we have measured the changes in surface area upon depositing Al_{13} on zeolite USY. The BET surface area was decreasing with increasing number of Al_{13} exchanges (x): $x = 0$ (738 m^2/g), 1 (714 m^2/g), 2 (687 m^2/g), and 5 (605 m^2/g), which suggests a partial blocking of the zeolite channel system with an increasing amount of Al_2O_3 coating. This is especially pronounced for the $[Al_{13}]_5$-USY material. Summarizing, it is important to notice that all these characterization results only confirm that aluminum is mainly deposited onto the outer surface of the zeolite Y. However, there is no clear evidence for lattice destruction or the presence of an extra Al_2O_3 phase, and the present data also do not provide any information about the exact location of the Al_2O_3 coating on the zeolite surface.

Figure 11A,B shows the ESR spectra of V^{4+}-impregnated $[Al_{13}]_x$-USY materials as a function of the amount of V^{4+} and the number of ion-exchange steps with Al_{13} (x). It is clear that the spectra consist of two overlapping spectra of V^{4+}, and the corresponding ESR parameters were obtained as follows: (1) separate simulation of the ESR spectra of V^{4+}/USY (S_z) and V^{4+}/Al_2O_3 (S_a) using the g and A values of Table 2, (2) sum of both spectra with an appropriate weight coefficient ($S = c_zS_z + c_aS_a$), and (3) comparison of the simulated spectrum (S) with the experimental one (E), followed by possible reevaluation of the starting variables, and reiteration. The obtained values of c_z and c_a for different $[Al_{13}]_x$-USY materials as a function of the V^{4+} content are summarized in Table 3. These values

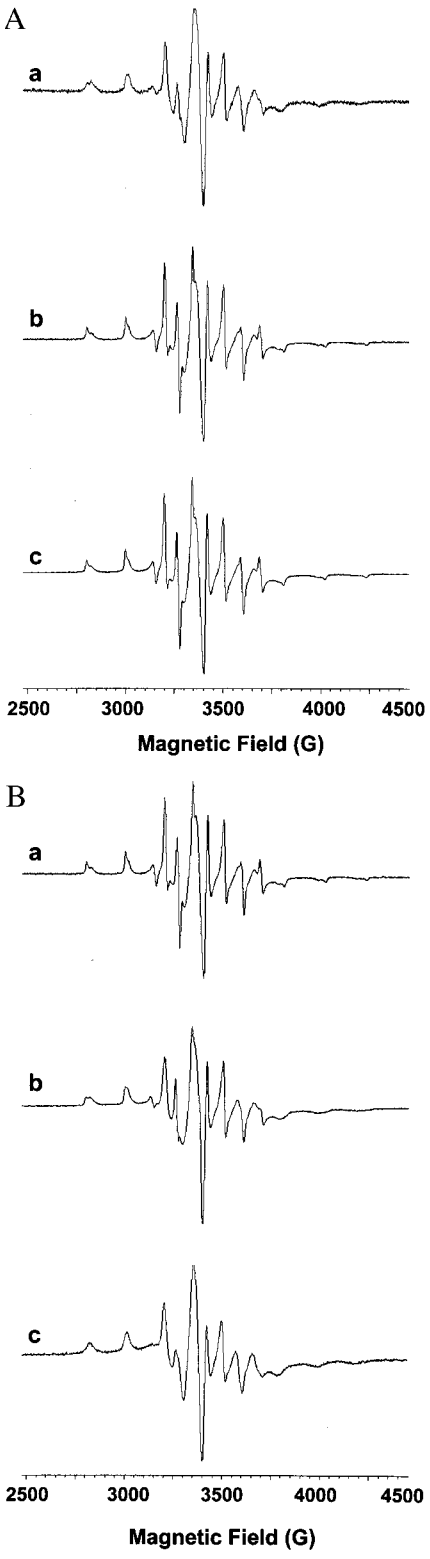

Figure 11. (A, top) ESR spectra of V^{4+}-impregnated $[Al_{13}]$-USY samples as a function of the V loading: (a) 0.05 wt %, (b) 0.10 wt %, and (c) 0.20 wt %. (B, bottom) ESR spectra of V^{4+}-impregnated $[Al_{13}]_x$-USY samples (V loading was 0.1 wt %) as a function of the number of Al_{13}-exchanges (x): (a) $x = 1$, (b) $x = 2$, and (c) $x = 5$.

indicate the preferential adsorption of V^{4+} onto the Al_2O_3 coating. This preferential adsorption is the most pronounced for the $[Al_{13}]_5$-USY sample. Finally, it is important to notice that the V^{4+} ions in these materials are well dispersed, which was evidenced by the linear increase of the intensity of the V^{4+} ESR signal with the V loading.

TABLE 3: ESR Parameters c_z and c_a for Different $[Al_{13}]_x$-USY Samples as a Function of the V Loading

no. of Al_{13} exchanges	V loading (wt %)	c_z	c_a
1	0.05	0.27	0.73
1	0.10	0.65	0.35
1	0.20	0.70	0.30
2	0.10	0.45	0.55
5	0.10	0.07	0.93

SCHEME 1: VO^{2+} Crystal Field Splitting Diagram

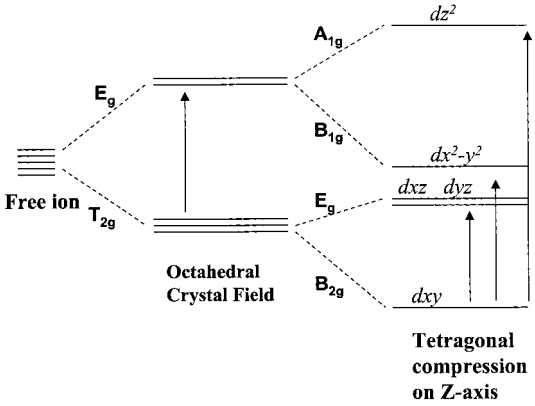

4. Discussion

1. Spectroscopic Fingerprinting. By careful simulating the ESR spectra, one can extract reliable and useful spin-Hamiltonian parameters from complex overlapping spectra, such as those reported in this work. The obtained values are summarized in Table 2, which are typical for a slightly rhombic symmetry of the coordination environment of V^{4+}. This rhombicity is the most pronounced for the V^{4+}/SiO_2 sample. Due to the goodness of fit, these reported values can be compared with those of well-defined molecular complexes in the literature.[22−24]

The V^{4+} species described in this work have clear vanadyl character $[VO^{2+}]$, which means that one of the vanadium−oxygen bonds is particularly short and can be described in terms of a V═O bond. This species has also been previously studied by Raman spectroscopy, and its characteristic ν(V═O) frequency is located at around 995 cm^{-1}.[25,26] Thus, V^{4+} experiences a tetragonal compression on the z axis, and the unpaired electron is located in the $3d_{xy}$ orbital of the transition metal ion (Scheme 1).[18,27] Indeed, all the V^{4+} species are characterized by average values of g and A ($g_{iso} = (g_{xx} + g_{yy} + g_{zz})/3$ and $A_{iso} = (A_{xx} + A_{yy} + A_{zz})/3$) which, if plotted in the (A_{iso} vs g_{iso}) empirical correlation diagram proposed by Davidson and Che,[22] fall in the region of vanadyl species, i.e., the α zone. Such a diagram has been derived on the basis of the analysis of series of well-defined vanadyl complexes, and the α zone, in which our g_{iso} and A_{iso} values fall, is typical of 5- and 6-coordinated vanadyl species, i.e., $(VO^{2+})_{5c}$ and $(VO^{2+})_{6c}$, respectively. Both species are difficult to distinguish by EPR because the sixth ligand is only weakly interacting. In addition, characteristic for such complexes is that $g_\perp > g_{||}$, $A_\perp < A_{||}$, and $A_{iso} > 100$ G, which is indeed the case for V^{4+}/USY and V^{4+}/Al_2O_3 if we assume an average axial distortion, i.e., an average of g_{xx} (or A_{xx}) and g_{yy} (or A_{yy}).

These facts, together with the observation of pseudooctahedrally coordinated V^{4+} by DRS, point toward the presence of a distorted octahedral structure with one coordination vacancy along the other axial position. The latter vacancy is most probably filled by an additional water ligand or a lattice oxygen, which completes the coordination sphere. A pictorial repre-

SCHEME 2: Pictorial Representation of Coordination Geometry of VO^{2+} on a Support

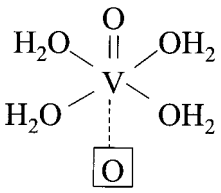

TABLE 4: Literature Survey of ESR Parameters of Supported Vanadium Oxide Catalysts[28−32]

catalyst	g_{xx}	g_{yy}	g_{zz}	A_{xx}	A_{yy}	A_{zz}
V−Y	1.986	1.986	1.938	74.9	74.9	190.6
VAPO-5	1.977	1.993	1.947	74.2	74.2	196
	1.977	1.992	1.930	74	74	195
$VOSO_4/Al_2O_3$	1.966	1.966	1.920	64.3	64.3	193.4
V_2O_5/ZSM-5	1.981	1.981	1.946	77	77	180
V/Aerosil-90	1.979	1.979	1.933	73.5	73.5	177
V−silicalite	1.994	1.994	1.935	69	69	183

sentation is given in Scheme 2. We assume then that the coordination by water or a lattice oxygen must be the most pronounced for V^{4+} on Al_2O_3 because the g and A values are close to axial symmetry. This is in line with calculations of $|\Delta g_\perp|$,

$$|\Delta g_\perp| = -2\lambda\epsilon_\pi^2\beta_2^{*2}/\Delta E_{xz/yz} \quad (3)$$

which is a measure of tetragonal distortion.[25] Here λ denotes the spin−orbit coupling parameter of the free vanadium ion ($\sim$170 cm^{-1}) and β_2^* and ϵ_π are molecular orbital (MO) coefficients, whereas $E_{xz/yz}$ is the excitation energy of the $B_{2g} \rightarrow E_g$ transition (Scheme 1). $E_{xz/yz}$ increases with tetragonal distortion, i.e., with a compression of the vanadium−oxygen distance along the z axis relative to the bond lengths in the xy plane (Scheme 1). The $|\Delta g_\perp|$ values, summarized in Table 2, suggest a shortening of the V=O bond for V^{4+}/Al_2O_3. Finally, Scheme 1 allows to assign the 770−805 and 580−625 nm DRS bands to a $B_{2g} \rightarrow E_g$ and $B_{2g} \rightarrow B_{1g}$ transition, respectively. The latter transition is equal to the ligand field strength $10Dq$, and close to values of $VO^{2+}(H_2O)_5^{2+}$ in aqueous solution (770 nm). The $B_{2g} \rightarrow A_{1g}$ transition, located at around 330−250 nm, is not well resolved because of the background of the support at around 200 nm.

It is also important to compare the g values of this work with some literature values, which are compiled in Table 4.[28−32] The latter values were mainly obtained by visual inspection of the ESR spectra. It is clear that up to now almost all the ESR spectra of V^{4+} on supports were explained in terms of an axial Hamiltonian H, i.e., with distinct $g_{||}$ ($A_{||}$) and $g_\perp$ ($A_\perp$) parameters. On the contrary, a rhombic component was always revealed in the ESR spectra by applying a detailed simulation procedure. This was previously also reported for VAPO-5 molecular sieves.[30] However, only high-frequency ESR (in W-band) will be able to resolve this issue in detail. Nevertheless, the obtained values for V/USY and V/Al_2O_3 are close to those previously reported for V/Y and $VOSO_4/Al_2O_3$, respectively, and only in the case of V/SiO_2 was a clearly rhombic symmetry detected, which is comparable with the Cr^{5+} (d^1) on SiO_2 system.[33]

The interpretation of the DRS spectra of supported V^{5+} ions is less straightforward. This is mainly due to the fact that DRS only probes the first coordination sphere around V^{5+}. Unlike Cr^{6+},[21,22,33] which only exists in tetrahedral coordination, V^{5+} can be present in both tetrahedral and octahedral coordination. In addition, both coordination geometries give rise to different degrees of polymerization. As a consequence, only limited information about the coordination geometries of V^{5+} can be extracted from the DRS spectra. In this respect, Raman spectroscopy is a much more powerful technique because the V−O and V=O vibrations of supported V^{5+} species can be easily studied.[34,35] Nevertheless, tetrahedral V^{5+} is always detected as the main species on Al_2O_3 at low loadings, which is in line with the observation of $VO_3(OH)^{2-}$ and $(VO_3)_n$ by Raman spectroscopy.[35] Only in the case of V^{5+}/USY and high loaded V^{5+}/SiO_2 samples was some polymerized $V^{5+}(O_h)$ detected. Thus, the V^{5+} speciation under ambient conditions is determined by the isoelectric point of the supports and in line with solution chemistry of V^{5+}.[35,36]

Finally, it is important to notice that combined DRS−ESR spectroscopies allow a quantitative determination of the amount of V^{4+} and V^{5+} ions on supports at least at low V loadings. At higher V loadings, the calibration lines deviate from linearity. This can be explained by (1) the inherent limitations of the Kubelka−Munk theory or (2) the multispeciation of V^{n+} species on the different supports. ESR seems to be the technique of choice for quantifying V^{4+} because of its well-resolved spectra.

2. Preferential Adsorption and Mobility. The series of mobility experiments described in this work illustrate the use of a well-defined set of spectroscopic fingerprints of supported V^{4+} and V^{5+} to study the preferences when different inorganic oxides are in competition for V^{n+} ions. In this respect, the favorite ion is V^{4+} because it can be studied by both DRS and ESR.

For the three physical mixtures under study, both V^{4+} and V^{5+} ions show the following preference order, $Al_2O_3 > SiO_2 \cong$ USY, and recently, the same preference sequence was observed for Cr^{n+} ions.[21] Thus, V^{n+} ions prefer the Al_2O_3 surfaces, and their migration toward Al_2O_3 is fast and easy via the adsorbed water phase. In the case of V^{5+}, the preferential adsorption of $VO_3(OH)^{2-}$ on Al_2O_3 can be easily explained by (1) the electrostatic attraction between $VO_3(OH)^{2-}$ and positively charged sites at the alumina surface ($Al-OH_2^+$) and (2) an acid−base reaction between $VO_3(OH)^{2-}$ and Al_2O_3. This surface reaction can be envisaged as follows:

$$VO_3(OH)^{2-} + Al-OH \leftrightarrow (Al-^+)[VO_3^-] + 2OH^- \quad (4)$$

The SiO_2 and USY surfaces are much more acidic, and thus the equilibrium of reaction 4 is more to the left, explaining the rather low preference for these supports. The preference of V^{4+} ions for Al_2O_3 surfaces can also be explained in terms of acid−base properties. Another interpretation is that an oxide ligand of Al_2O_3 is directly coordinating to VO^{2+} along the axial position (Scheme 2), giving rise to a stable coordination geometry.

3. Al_2O_3 Coating of Zeolite Y. The adsorption of Al_{13} on NaY results in a maximum adsorption of 0.88 mmol Al/g, i.e., 0.07 mmol Al_{13}^{7+} cations. Thus, the exchange level is estimated to be equal to about 14% of the cation exchange capacity (CEC), which is too high to be solely attributed to a pure $Na^+ \leftrightarrow Al_{13}^{7+}$ exchange. A similar reasoning can be made for the ion-exchange process of Al_{13} on USY. As a consequence, supplementary reactions, such as proton exchange and the reaction of Al_{13}^{7+} with hydroxyl groups, are involved in this coating process.

Calcination will result in a decomposition of the Al_{13} ion, according to

$$2[Al_{13}O_4(OH)_{24}(H_2O)_{12} \rightarrow 13Al_2O_3 + 41H_2O + 14H^+ \quad (5)$$

Indeed, the observation that $V^{4+}/[Al_{13}]_x$-USY samples have a

characteristic ESR spectrum of V^{4+} on Al_2O_3 points toward the presence of Al_2O_3 particles. Other evidence for the presence of Al_2O_3 particles comes from ^{27}Al MAS NMR and electron microprobe surface analysis. The Al_2O_3 particles are most probably located at the outer surface of the zeolite, although their exact location is not yet known. We anticipate that the number and size of these particles grow with successive Al_{13} exchanges and calcinations. However, one cannot rule out the possibility that some Al^{3+} will diffuse into the zeolite channels. Indeed, our N_2 adsorption studies indicate a small decrease of the surface area of zeolite USY. As a consequence, further studies will be focused on the detailed interaction mechanism between Al_2O_3 and zeolite USY.

5. Conclusions

We have shown that combined DRS−ESR spectroscopies are suitable techniques (a) to unravel the coordination geometry of supported V^{n+} species ($n = 4$ and 5), (b) to quantify the amount of supported V^{n+} species at low V loadings, and (c) to study the mobility and the preference orders of V^{n+} in SiO_2, Al_2O_3, and USY and their physical mixtures. The following conclusions can be made:

(1) V^{4+} is present on SiO_2, Al_2O_3, and USY surfaces as a distorted octahedral species. This species has a strong vanadyl character and possesses one coordination vacancy that is filled by either a water molecule or an oxygen atom of the support.

(2) Supported V^{5+} species are always in tetrahedral coordination, although some polymerized $V^{5+}(O_h)$ is observed in USY and V^{4+}/SiO_2 samples with higher V loadings.

(3) Both V^{4+} and V^{5+} ions are mobile on hydrated surfaces and preferentially adsorb on Al_2O_3.

(4) The external surface of USY can be coated with a thin film of Al_2O_3, which preferentially adsorbs V^{4+} ions. The method is based on the ion exchange of USY with the Keggin ion, $[Al_{13}O_4(OH)_{24}(H_2O)_{12}]^{7+}$.

(5) ESR is the technique of choice for probing the coordination environment and quantifying the amount of V^{4+} on inorganic oxides.

Acknowledgment. This work was supported in the frame of a cooperation program between the Ministry of the Flemish Community (Belgium) and the Ministry of Research and Technology (Romania). R.R. thanks the Research Council of K.U. Leuven for a junior postdoctoral fellowship. B.M.W. and P.V.D.V. are postdoctoral fellows of the Fonds voor Wetenschappelijk Onderzoek (F.W.O.). The authors thank Prof. Israel Wachs (Lehigh University, USA) for supplying the reference vanadium oxide compounds, Ms. Fina Pelgrims for performing SEM measurements, and Prof. Piet Grobet and Bart Wauters for the NMR measurements.

References and Notes

(1) Wainwright, M. S.; Foster, N. R. *Catal. Rev.—Sci. Eng.* **1979**, *19*, 211.

(2) Nikolov, V.; Klssurski, D.; Anastasov, A. *Catal. Rev.—Sci. Eng.* **1991**, *33*, 1.

(3) Sanai, M.; Anderson, A. *J. Mol. Catal.* **1990**, *59*, 233.

(4) Bosch, H.; Janssen, F. *Catal. Today* **1988**, *2*, 369.

(5) Svachula, J.; Alemany, L. J.; Feriazzo, P.; Tronconi, E.; Bregani, F. *Ind. Eng. Chem. Res.* **1993**, *32*, 826.

(6) Harding, W.; Birkeland, K. E.; Kung, H. H. *Catal. Lett.* **1994**, *28*, 1.

(7) Forzatti, P.; Tronconi, E.; Busca, G.; Tittarelli, P. *Catal. Today* **1987**, *1*, 209.

(8) Woltermann, G. M.; Magee, J. S.; Griffith, S. D. *Stud. Surf. Sci. Catal.* **1993**, *76*, 105.

(9) Yang, S. J.; Chen, Y. W.; Li, C. *Appl. Catal. A: Gen.* **1994**, *115*, 59.

(10) Trujillo, C. A.; Knops-Gerrits, P. P.; Orieda, L. A.; Jacobs, P. A. *J. Catal.* **1997**, *168*, 1.

(11) Wachs, I. E.; Weckhuysen, B. M. *Appl. Catal. A: Gen.* **1997**, *157*, 67.

(12) Schoonheydt, R. A. In *Characterization of Heterogeneous Catalysts*; Delannay, F., Ed.; Marcel Dekker: New York, 1984; p 125 and references therein.

(13) Weckhuysen, B. M.; Schoonheydt, R. A. *Catal. Today* (submitted for publication), and references therein.

(14) Weckhuysen, B. M.; Heidler, R.; Schoonheydt, R. A. In *Molecular Sieves—Science and Technology*; Karge, H., Weitkamp, J., Eds.; Springer-Verlag: Berlin (in press), and references therein.

(15) Furrer, G.; Ludwig, C.; Schindler, P. W. *J. Colloid Interface Chem.* **1992**, *149*, 56.

(16) Schoonheydt, R. A.; Leeman, H.; Scorpion, A.; Lenotte, I.; Grobet, P. *Clays Clay Miner.* **1994**, *42*, 518.

(17) The QPOW simulation program can be obtained from Dr. Marc Nilges of the Illinois EPR Research Center. This program generates a powder spectrum for a spin $^1/_2$ or greater with one metal nucleus (calculated to full order: matrix diagonalization with up to a fourth-order perturbation to convert from frequency domain to field domain) and two superhyperfine spins for which there can be more than one equivalent nucleus.

(18) Ballhausen, C. J.; Gray, H. B. *Inorg. Chem.* **1962**, *1*, 111.

(19) Lever, A. B. P. *Inorganic Electronic Spectroscopy*, 2nd ed.; Elsevier: Amsterdam, 1984.

(20) Greenwood, N. N.; Earnshaw, A. *Chemistry of the Elements*; Pergamon Press: Oxford, 1984.

(21) Weckhuysen, B. M.; Schoofs, B.; Schoonheydt, R. A. *J. Chem. Soc., Faraday Trans.* **1997**, *93*, 2117.

(22) Davidson, A.; Che, M. *J. Phys. Chem.* **1992**, *96*, 9909.

(23) Mabbs, F. E. *Chem. Soc. Rev.* **1993**, 314.

(24) Mabbs, F. E.; Collison, D. *Electron Paramagnetic Resonance of d Transition Metal Compounds*; Elsevier: Amsterdam, 1992.

(25) Walther, K. L.; Schraml-Marth, M.; Wokaun, A. *Catal. Lett.* **1990**, *4*, 327.

(26) Cristiani, C.; Forzatti, P.; Busca, G. *J. Catal.* **1989**, *116*, 586.

(27) Ophardt, C. E.; Stupgia, S. *J. Chem. Educ.* **1984**, *61*, 1102.

(28) Whittington, B. I.; Anderson, J. R. *J. Phys. Chem.* **1993**, *97*, 1032.

(29) Martini, G.; Ottaviani, M. F.; Seravilli, G. L. *J. Phys. Chem.* **1975**, *79*, 1716.

(30) Weckhuysen, B. M.; Vannijvel, I. P.; Schoonheydt, R. A. *Zeolites* **1995**, *15*, 482.

(31) Centi, G.; Perathoner, S.; Trifiro, F.; Aboukais, A.; Aissi, C. F.; Guelton, M. *J. Phys. Chem.* **1992**, *96*, 2617.

(32) Vedrine, J. C. In *Characterization of Heterogeneous Catalysts*; Delannay, F., Ed.; Marcel Dekker: New York, 1984; p 78.

(33) Weckhuysen, B. M.; Wachs, I. E.; Schoonheydt, R. A. *Chem. Rev.* **1996**, *96*, 3327.

(34) Deo, G.; Wachs, I. E.; Haber, J. *Critic. Rev. Surf. Chem.* **1994**, *4*, 141.

(35) Deo, G.; Wachs, I. E. *J. Phys. Chem.* **1991**, *95*, 5889.

(36) Baes, C. F., Jr.; Mesmer, R. E. *The Hydrolysis of Cations*; Wiley: New York, 1970.